Published in final edited form as:
IEEE Trans Ultrason Ferroelectr Freq Control. 2013 November ; 60(11): 2257–2265. doi:10.1109/TUFFC.2013.6644731.

Dependence of the Reversibility of Focused-Ultrasound-Induced Blood–Brain Barrier Opening on Pressure and Pulse Length *In Vivo*

Gesthimani Samiotaki and
Department of Biomedical Engineering, Columbia University, New York, NY

Elisa E. Konofagou
Department of Radiology, Columbia University, New York, NY

Gesthimani Samiotaki: gs2496@columbia.edu

Abstract

The most challenging aspect of intravenously-administered drugs currently developed to treat central nervous system (CNS) diseases is their impermeability through the blood–brain barrier (BBB), a specialized vasculature system protecting the brain microenvironment. Focused ultrasound (FUS) in conjunction with systemically administered microbubbles has been shown to open the BBB locally, noninvasively, and reversibly. The objective of this study was to investigate the effect of FUS (center frequency: 1.5 MHz) pulse length (PL), ranging here from 67 μs to 6.7 ms, on the physiology of the FUS-induced BBB opening. Dynamic contrast-enhanced (DCE) and T1-weighted magnetic resonance imaging (MRI) were used to quantify the permeability changes using transfer rate (K_{trans}) mapping, the volume of BBB opening (V_{BBB}) and the reversibility timeline of the FUS-induced BBB opening, with the systemic administration of microbubbles at different acoustic pressures, ranging from 0.30 to 0.60 MPa. Permeability and volume of opening were both found to increase with the acoustic pressure and pulse length. At 67-μs PL, the opening pressure threshold was 0.45 MPa, with BBB opening characteristics similar to those induced with 0.60 MPa at the same PL, as well as with 0.67-ms PL/0.30 MPa. On average, these cases had $K_{trans} = 0.0049 \pm 0.0014$ min^{-1} and $V_{BBB} = 3.7 \pm 4.3$ mm^3, and closing occurred within 8 h. The 6.7-ms PL/0.30 MPa induced similar opening with 0.67-ms PL/0.45 MPa, and a closing timeline of 24 to 48 h. On average, K_{trans} was 0.0091 ± 0.0029 min^{-1} and V_{BBB} was 14.13 ± 7.7 mm^3 in these cases. Also, there were no significant differences between the 6.7-ms PL/0.45 MPa, 0.67-ms PL/0.60 MPa and 6.7-ms PL/0.60 MPa cases, yielding on average a K_{trans} of 0.0100 ± 0.0023 min^{-1} and V_{BBB} equal to 20.1 ± 5.7 mm^3. Closing occurred within 48 to 72 h in these cases. Stacked histograms of the K_{trans} provided further insight to the non-uniform spatial distribution of permeability changes and revealed a correlation with the closing timeline. These results also suggest a beneficial complementary relationship between the elongation of the PL and the decrease of the peak negative acoustic pressures, and vice versa. Linear regression between K_{trans} and V_{BBB} showed a good correlation fit. Also, the time required for closing linearly increased with V_{BBB}. The volume rate of decrease was measured to be 11.4 ± 4.0 mm^3 per day, suggesting that the closing timeline could be predicted from the initial volume of opening. Finally, no histological damage was detected in any of the cases 7 d post-FUS, indicating the safety of the methodology and parameters used.

I. Introduction

In order for central nervous system (CNS) diseases to be treated noninvasively, it is mandatory to transport therapeutic agents across the specialized vascular system lining the cerebral microvessels, the blood–brain barrier (BBB), which consists of endothelial cells

connected together by tight junctions, as well as astrocytes, neurons, microglia, and pericytes [1], [2]. The BBB is a metabolic and physical barrier, which constrains the passage of molecules to the brain, either through paracellular or transcellular pathways [2], unless they are both lipid-soluble and of a molecular weight (MW) lower than 400 D a [3]. It has been demonstrated that focused ultrasound (FUS) in conjunction with intravenously administered microbubbles can successfully open the BBB noninvasively, locally, and reversibly [4]–[7].

Despite the fact that the mechanism of FUS-induced BBB opening remains unknown, several studies have been conducted to investigate the influence of several acoustic parameters, such as the frequency [8], [9], pulse repetition frequency (PRF) [10]–[12], sonication duration [9], [13], microbubble size [14]–[17], and pulse length [10]–[12]. Moreover, it has been reported that the BBB opening can be achieved with short pulse lengths (PLs) as low as 33 μs [11] at 0.46 MPa and 10 Hz PRF, or even with 2.3-μs pulses transmitted with the higher PRF of 100 Hz and higher pressure of 0.51 MPa [12], which were also found to facilitate a more spatially uniform distribution of the delivered fluorescently tagged dextrans. It has also been reported that increased number of cycles within a given pulse length (10 ms) correlated with edema without significantly increasing the enhancement of the tracer delivery [18]. However, the effect of the pulse length on the transfer rate from blood to tissue parenchyma and the corresponding permeability maps, as well as the volume and the duration or reversibility of the BBB opening, have not been studied thus far.

Recently, some physiological characteristics of the FUS-induced BBB opening, i.e., the *in vivo* permeability changes [15], [19], the volume of opening, and the reversibility timeline [16], have been investigated with the use of dynamic contrast-enhanced magnetic resonance imaging (DCE-MRI) and T1-weighted magnetic resonance (MR) images with gadodiamide (MW: 574 Da, Omniscan, GE Healthcare, Little Chalfont, UK) as a tracer, and mono-disperse microbubbles (1 to 2, 4 to 5, and 6 to 8 μm in diameter) at a pulse length of 0.67 ms, showing a dependence on the acoustic pressure and the microbubble size used. Definity microbubbles, which have been widely used in FUS-induced BBB opening studies, are highly polydisperse in size, containing a range of diameters from less than 1 μm to 10 μm, but with most of the microbubbles ranging below 2 μm in diameter [20], [21]. The bioeffects of this particular polydisperse agent, i.e., Definity, compared with what has been previously reported for the isolated mono-dispersed microbubbles were also studied here.

The objective of this study was thus to investigate the effect of FUS *in vivo* on the BBB opening physiology, using a range of pulse lengths, varying from 67 μs to 6.7 ms at a PRF of 10 Hz, while also varying the acoustic pressure between 0.30 MPa and 0.60 MPa, to study their effect on the FUS-induced BBB opening *in vivo*. Gadodiamide was used as the tracer to depict BBB opening for the acquisition of DCE-MRI and T1-weighted MR images to measure the permeability changes and maps, in order to quantify the volume of opening and determine the reversibility timeline of BBB opening. Moreover, another objective of this study is to investigate the relation between permeability changes, volume of opening, and the time required for BBB closing, with the goal of establishing a correlation, which could potentially be used to predict the time required for closing. Finally, the safety of the procedures and the acoustic parameters used was assessed through histological analysis.

II. Materials and Methods

A. Ultrasound

A single-element, spherical-segment FUS transducer (center frequency: 1.5 M Hz, focal depth: 60 mm, radius: 30 mm; Imasonic SAS, Voray-sur-l'Ognon, France), driven by a

function generator (Agilent Technologies Inc., Santa Clara, CA) through a 50-dB power amplifier (Electronic Navigation Industries, Rochester, NY). A central void of the therapeutic transducer held a pulse-echo ultrasound transducer (center frequency: 10 M Hz, focal depth: 60 mm, radius 11.2 mm; Olympus NDT, Waltham, MA) used for alignment, with their two foci aligned. The imaging transducer was driven by a pulser-receiver (Olympus NDT) connected to a digitizer (Gage Applied Technologies Inc., Lachine, QC, Canada). A cone filled with degassed and distilled water was mounted onto the transducer assembly. The transducers were attached to a computer-controlled 3-D positioning system (Velmex Inc., Lachine, QC, Canada); see Fig. 1. The FUS focal spot and the axial and lateral full-width at half-maximum intensities were 7.5 mm and 1 mm, respectively, overlapped with the right hippocampus and the lateral portion of the thalamus. 1 μL/g of body mass of Definity microbubbles, 1:20 diluted in phosphate buffered saline (PBS), was intravenously injected immediately preceding the sonication. Thirty-six ($n = 36$) wild-type adult male mice (strain: C57BL/6, Harlan Sprague Dawley, Indianapolis, IN) were sonicated for 60 s, with a pulse rate of 10 Hz, at peak negative acoustic pressures (PNPs) of 0.30, 0.45, and 0.60 MPa, after accounting for 18% murine skull attenuation [5]. A sham group of three mice underwent the whole procedure without FUS. All mouse experiments were carried out in accordance with the Columbia University Institutional Animal Care and Use Committee. The PLs tested were 67 μs, 0.67 ms, and 6.7 ms. The acoustic pressures were obtained experimentally in a degassed water tank. A needle hydrophone (HGL-0400, Onda Corp., Sunnyvale, CA) was used for the transducer calibration, which measured the acoustic pressure in a tank filled with degassed water. The mice were anesthetized using 1.25% to 2.50% isoflurane (SurgiVet, Smiths Medical PM Inc., Waukesha, WI) mixed with oxygen during the experiments.

B. Magnetic Resonance Imaging

All mice were imaged using a 9.4-T microimaging MRI system (DRX400, Bruker Biospin, Billerica, MA). Each mouse was scanned 30 to 40 min after sonication, using a 30-mm-diameter 1H resonator. Isoflurane gas (1% to 2%) was used to keep the mouse anesthetized at 50 to 70 breaths/min during the entire MRI procedure. On the day of sonication (Day 0), DCE-MRI was performed using a 2-D FLASH T1-weighted sequence (192 × 128 matrix size, spatial resolution of 130 × 130 μm^2, slice thickness of 600 μm, TR/TE = 230/2.9 ms). During the third acquisition of the dynamic sequence, a 0.30-mL undiluted bolus of gadodiamide (Omniscan) was injected intraperitoneally (IP) and was used as a tracer to depict the area of opening. This large dose ensured the presence of a bolus peak in the blood circulation in the vasculature, which is required for the arterial input function determination, and ensured a sufficient amount for the depiction of the BBB opening. After the completion of DCE-MRI, a post-contrast enhancement, T1-weighted 2-D FLASH high-resolution acquisition (TR/TE: 230/3.3 ms, resolution 100 × 100 μm, slice thickness: 400 μm) was acquired. The scanning times of each DCE and T1-weighted MRI image were 40 min and 4 min respectively. Pre- and post-contrast T1-weighted MR imaging was repeated on a daily basis starting from the day of sonication (1 h) and lasting up to 72 h after sonication. Mice with a small detectable opening were also imaged 8 h after sonication. The general kinetic model (GKM) [22] was used to measure the BBB permeability to Omniscan in the targeted region, as described elsewhere [15], providing maps of K_{trans} (Fig. 2), which denotes the transfer rate from the blood plasma to the extravascular extracellular space of each voxel. The arterial input function (AIF) was determined by averaging the gadodiamide concentration changes in the internal carotid artery from the entire cohort of wild-type mice. The average of all K_{trans} values of the voxels in a 3-D volume of interest (VOI) of 52 mm^3, overlapping with the targeted area and the entire focal spot which did not exceed the brain volume, was calculated and was used for the quantitative K_{trans} plot for all groups, as shown in Fig. 3. Stacked K_{trans} histograms in the same VOIs were also created to provide more

quantitative information on the relative changes in K_{trans} within the VOI, as shown in Fig. 4. The average K_{trans} was also measured in the nonsonicated contralateral side of the VOI and in the sham group, and was used as a reference, i.e., a baseline K_{trans} of the brain tissue around the hippocampal area without any BBB disruption. The volume of opening (V_{BBB}) was quantified by thresholding voxels within the VOI with signal intensity (S.I.) of 2.5 standard deviations or above the S.I. of a reference region in the nonsonicated area, while the volume of contrast-enhanced vasculature was excluded; those longitudinal measurements are shown in Fig. 5.

C. Safety Assessment

On day 7 after the FUS-induced BBB opening, all mice were euthanized and transcardially perfused with 30 mL of PBS and 60 mL of 4% paraformaldehyde. Heads were soaked in paraformaldehyde for 24 h. Skulls were removed, and the brains were fixed again in 4% paraformaldehyde for 6 d, followed by conventional post-fixation procedures. The paraffin-embedded specimens were sectioned horizontally at a thickness of 6 μm. For each brain, there were 32 sections prepared, with 100 μm spacing between planes. Sections were stained with hematoxylin and eosin (H&E) and then the sections that included the hippocampus (i.e., the region with highest MRI enhancement or opening) at the sonicated level were examined for red blood cell extravasations into the brain parenchyma as well as cell loss.

D. Statistical Analysis

The measurements in the sham group were used to determine whether the integrity of BBB was fully restored in the BBB-opened cases, as described by Samiotaki *et al*. [16]. Following the calculation of the mean and standard deviation of the volumetric measurements for each group, a two-tailed Student's *t*-test was performed between the FUS group and the sham group, and if no statistically significant difference was observed ($p > 0.05$), then the BBB was considered to have been restored.

Comparison among different groups that received sonication was also performed, using a two-tailed Student's *t*-test, to reveal any statistically significant differences ($p < 0.05$) resulting from the different acoustic parameters used for both the quantitative measurements of K_{trans} and volume of opening.

III. Results

Horizontal MR images overlaid with K_{trans} maps are shown in Fig. 2, for all PLs and PNPs used, followed by longitudinal high-resolution T1-weighted MR images showing BBB opening. White font color denotes closing, and images following detected closing confirm that BBB remained closed. The K_{trans} maps show the nonuniformity of the spatial distribution in permeability changes in each combination of PL and PNP studied. The progress of BBB opening to closing is shown in the T1-weighted images; signal enhancement resulting from the diffusion of gadodiamide through the opened BBB depicts the opening area. BBB closing followed a radial inward pattern toward the center of the FUS beam, in agreement with previous findings [16]. At 67-μs PL, 0.30 MPa was found not to be sufficient to induce detectable opening, and for 0.45 MPa and 0.60 MPa closing occurred within 8 h after opening. At 0.67-ms PL closing occurred within 8 h for 0.30 MPa, within 24 h for 0.45 MPa, and within 24 to 48 h for 0.60 MPa. Finally, at 6.7-ms PL, closing occurred within 24 to 48 h for 0.30 MPa, and within 48 to 72 h for both 0.45 and 0.60 MPa.

The permeability average K_{trans} values of the 3-D VOI which was overlapping with the right hippocampus, as provided by quantitative measurements, are shown in Fig. 3. The dotted-line bar represents the average K_{trans} of the sham group which was measured to be 0.0038 ±

0.001 min^{-1}. This nonzero value is generated by noise in the calculation from the vasculature and ventricles where gadolinium naturally flows. At 0.30 MPa, a 67-μs PL did not cause any increase in permeability compared with the baseline, a 0.67-ms PL increased K_{trans} to 0.0050 ± 0.0013 min^{-1} and a 6.7-ms PL increased K_{trans} to 0.0092 ± 0.0023 min^{-1}. At 0.45 MPa, a 67-μs PL increased K_{trans} slightly above the baseline to 0.0036 ± 0.0008 min^{1}, but compared with the shortest PL, both 0.67-ms and 6.7-ms PLs significantly increased K_{trans}, to 0.0097 ± 0.0026 min^{-1} and 0.0111 ± 0.0027 min^{-1}, respectively. At 0.60 MPa, K_{trans} was increased to 0.0057 ± 0.0015 min^{-1} at 6.7-μs PL, and then to 0.0101 ± 0.0017 min^{-1} and 0.098 ± 0.0119 min^{-1} for 0.67- and 6.7-ms PLs, respectively. Statistical significance was found between the 67-μs PL and the 6.7-ms PL at 0.30 MPa ($p < 0.05$), as well as between the 67-μs PL and both the 0.67-ms and 6.7-ms PL ($p < 0.05$) at 0.45 MPa ($p < 0.05$).

Further analysis of the distribution of permeability changes within the opening volume (Fig. 4) provided further insight to the observed phenomenon of cases with non-significantly different average K_{trans} having different closing timelines. The relationship between the nonuniform changes in permeability as revealed in the K_{trans} maps, PL, and PNP is quantified in the stacked histograms of K_{trans} shown in Fig. 4. At 0.30 MPa, the volume of the blue cluster (0.006 to 0.015 min^{-1}) K_{trans}, as well as the volume of the green cluster (0.016 to 0.025 min^{-1}) K_{trans}, were increased 3-fold when PL was 0.67 ms, and 8-fold when it was 6.7 ms, compared with baseline volume, i.e., compared with 67 μs, for which no opening was detected. There was some increase in the volume of the yellow K_{trans} cluster (0.026 to 0.035 min^{-1}) and the orange cluster (0.036 to 0.045 min^{-1}), but no difference in the red K_{trans} cluster (0.046 to 0.060 min^{-1}). At 0.45 MPa, the volume of all permeability clusters increased more linearly with the increase of PL from 67 μs to 0.67 ms and then to 6.7 ms.

Quantitative volumetric measurements and the BBB opening reversibility timeline are shown in Figs. 5(a), 5(b), and 5(c) for 0.30, 0.45, and 0.60 MPa, respectively. More specifically, at 67 μs, V_{BBB} of 1.0 ± 1.4 mm^3 at 0.30 MPa (not opened – similar to sham), 2.6 ± 1.6 mm^3 at 0.45 MPa, and 6.9 ± 5.7 mm^3 at 0.60 MPa were induced, and the BBB closed within 8 h after opening. At a 0.67 ms pulse length, V_{BBB} initially induced was as low as 1.4 ± 0.5 mm^3 at 0.30 MPa and closing also occurred within 8 h, but V_{BBB} increased to 18.3 ± 8.0 mm^3 at 0.45 MPa and 19.9 ± 5.3 mm^3 at 0.60 MPa; closing occurred within 24 to 48 h for these pressures. At a 6.7 ms pulse length, V_{BBB} initially induced was 9.9 ± 5.7 mm^3 at 0.30 MPa, 23.9 ± 9.2 mm^3 at 0.45 MPa, and 19.3 ± 5.6 mm^3 at 0.60 MPa; closing occurred within 24 to 48 h at 0.30 MPa and within 48 to 72 h at the higher pressures. In addition, the volume decay rate was measured to be 11.4 ± 4.0 mm^3 per day, whereas any BBB opening below that value closed within the first 24 h or less.

The combination of the results with the data processing methods as shown in Figs. 3, 4, and 5 as well as statistical analysis revealed a trade-off between PL and PNP. At 67-μs PL, the opening pressure threshold was 0.45 MPa, with BBB opening characteristics similar to those induced with 0.60 MPa at the same PL, as well as with 0.67-ms PL/0.30 MPa. On average, these cases had K_{trans} = 0.0049 ± 0.0014 min^{-1} and V_{BBB} = 3.7 ± 4.3 mm^3, and closing occurred within 8 h. The 6.7-ms PL/0.30 MPa induced similar opening with 0.67-ms PL/0.45 MPa, and a closing timeline of 24 to 48 h. On average, K_{trans} was measured to be 0.0091 ± 0.0029 min^{-1} and V_{BBB} equal to 14.13 ± 7.7 mm^3 for these cases. Also, there were no significant differences between the 6.7-ms PL/0.45 MPa, 0.67-ms PL/0.60 MPa and 6.7-ms PL/0.60 MPa, yielding on average a K_{trans} of 0.0100 ± 0.0023 min^{-1} and V_{BBB} equal to 20.1 ± 5.7 mm^3. Closing occurred within 48 to 72 h for these cases.

The correlation between K_{trans}, V_{BBB}, and the time required for closing was also investigated and shown in this study. Good correlation between the time required for closing and the V_{BBB} on day 0 of opening is shown in Fig. 6. The time required for closing was found to monotonically increase with the volume of BBB opening induced on the day of FUS, and a linear regression fit showed a correlation of $R^2 = 0.78$, suggesting that the time required for closing could be predicted based on the volume of opening initially induced. Fig. 7 shows the average K_{trans} measured 1 h after sonication as a function of time required for closing, revealing that the average K_{trans} is deemed less reliable for closing prediction. Specifically, cases with non-significant statistical differences in their corresponding K_{trans}, were found to have different closing timelines—varying, for example, between 24 and 72 h. As may be expected, when the K_{trans} and the 1-h-post-sonication V_{BBB} were averaged within the same 52-mm^3 VOI, they were found to be linearly correlated (Fig. 8; $R^2 = 0.74$).

There was no damage detected under histological examination with H&E staining indicating that the parameters used were safe. An example is shown in Fig. 9.

IV. Discussion

In this study, properties of the FUS-induced BBB opening, i.e., permeability (K_{trans}), volume of opening (V_{BBB}), and the reversibility timeline, were assessed to determine the effect of the PL and the acoustic PNP on the restoration of the barrier. K_{trans}, V_{BBB}, and reversibility timeline were shown to be dependent on the PL and PNP. The PNP threshold for BBB opening was shown here to be dependent on the PL. A PL of 67 μs at 0.45 and 0.60 MPa induced BBB opening with similar K_{trans}, V_{BBB}, and closing timeline (8 h) with that induced by a 0.67-ms-PL at 0.30 MPa. A PL of 6.7 ms at 0.30 MPa induced a BBB opening with characteristics similar to those induced by a 0.67-ms-PL at 0.45 MPa, with a 24 to 48 h closing timeline. A PL of 6.7 ms at 0.45 or 0.60 MPa and 0.67 ms and 0.60 MPa also induced BBB opening with similar K_{trans} and V_{BBB} and closing timeline varied within 48 to 72 h. The time required for closing increased monotonically with the volume of opening [16], and was shown to follow a decay rate of 11.4 ± 4.0 mm^3 per day. The K_{trans} averaged in the whole sonicated BBB region was linearly correlated to the V_{BBB} on the day of sonication. Finally, there was no histological damage detected, indicating that the parameters tested here are safe.

An interesting finding is that at 0.30 MPa, the BBB opening occurred at the pulse length threshold of 0.67 ms with the BBB opening volume increasing with the pulse length beyond that value. It has been shown that inertial cavitation occurs at the pressures of 0.45 and 0.60 MPa but not at 0.30 MPa [23]. In the absence of inertial cavitation, the microbubbles may undergo stable or unstable oscillations, possibly leading to bubble growth through rectified diffusion or shrinkage leading to dissolution. The results shown here suggest that at 0.30 MPa with a pulse length of 67 μs emitted at 1.5 M Hz and a PRF of 10 Hz was not sufficient to mechanically engage the capillary walls, disrupt the blood–brain barrier, and cause diffusion of gadodiamide thereafter. Definity microbubbles were used in this study, which are polydispersed, with a mean diameter of 1.1 to 3.3 μm, which is comparatively smaller than the brain capillary mean diameter (4 to 10 μm), and thus induced opening only when the pulse length was increased to 0.67 ms and beyond. Therefore, it could be assumed that the duration of mechanical stress exerted on the capillary walls during each pulse must be sustained over a sufficient period of time to induce BBB opening.

Another interesting finding is that there were no significant differences between 0.45 and 0.60 MPa in the closing timeline with the longest PL, i.e., 6.7 ms [Fig. 2(c)]. This finding indicates that, because the effect on the BBB opening volume and duration is not affected by

the increase in the acoustic pressure from 0.45 MPa to 0.60 MPa, higher acoustic pressures should be avoided to achieve homogeneity of molecular diffusion.

At higher PNPs (0.45 and 0.60 MPa), despite the fact that the BBB opening characteristics (K_{trans}, V_{BBB}, and closing timeline) were similar between the 0.67-ms and 6.7-ms PLs, they were entirely different compared with the 67-μs PL. It has been shown that, at 0.45 and 0.60 MPa, the microbubbles undergo inertial cavitation [23], which means that the microbubbles expand several times to their equilibrium radii and then collapse. This, therefore, implies that because of the inertial cavitation, the microbubble activity and interaction with the capillary walls were significantly enhanced during a PL of 0.67 ms compared with a PL of 67 μs, and also, there was not much difference induced compared with 6.7 ms. Therefore, the assumption that can be made here is that inertial cavitation is not fully exploited at very short non-burst PL (i.e., 67 μs) and that after 0.67 ms, all bubbles would likely be destroyed, with additional cycles becoming redundant.

It is interesting that the K_{trans} histograms (Fig. 4) were quite similar among the PL/PNPs combinations that had similar closing timelines. For example, despite the fact that the average K_{trans}, as shown in Fig. 3, is the same among several groups, only the groups that had an increased volume with very high K_{trans} (yellow, orange, and red clusters) required more time for BBB restoration. It was shown that at the highest pressure, i.e., 0.60 MPa, the increase to the longest PL did not contribute to any significant permeability distributional changes in the BBB opening, i.e., 0.67 ms versus 6.7 ms PL, resulting in a closing timeline of 48 to 72 h. These cases were also similar to the 6.7-ms PL/0.45-MPa case in terms of BBB opening characteristics (K_{trans}, V_{BBB}, and closing timeline). At a given low pressure, the increase of PL had the same effect on permeability changes as that of a shorter PL at a higher pressure, for example the 6.7-ms PL/0.30-MPa and the 0.67-ms PL/0.45-MPa cases, having a closing timeline of 24 to 48 h. Finally, at a given short PL, the PNP had to be increased to induce opening similar to that of a longer PL at a lower PNP, i.e., 67-μs/0.45-MPa and 0.60 MPa versus 0.67-ms/0.30-MPa, and closing occurred within 8 h. These findings suggest that the time required for closing is strongly dependent on the volume that has highly increased permeability after FUS. Also, in the aforementioned cases, the fact that the BBB opening induced with the use of a low PNP with a long PL was similar to that induced by a higher PNP with a shorter PL suggests that there is a beneficial complementary relationship between the increase of the PL and the decrease of the PNP, and vice versa.

As previously mentioned, it has been shown that the BBB opening acoustic pressure threshold is pulse-length-dependent [10]–[12], [18]. However, the underlying BBB characteristics, such as the permeability, volume of opening, and reversibility timeline, had not been investigated until now. First, McDannold *et al.* [10] have also shown that the acoustic threshold pressure for BBB opening is pulse-length-dependent. Testing was performed with mainly longer pulse lengths than the ones used here, and more specifically, at 1-Hz PRF (at 0.69 M Hz, with Optison), BBB opening threshold was at 0.60, 0.47, and 0.36 MPa for 0.1, 1, and 10 ms pulse lengths, respectively. Moreover, using closely-timed short pulses, O'Reilly *et al.* [18] reported a semi-log relationship between the MR enhancement and the number of burst cycles, with a minimum of a 3-μs burst at 1 Hz (1.18 M Hz center frequency, Definity microbbubles) required to induce opening which is in agreement with the results shown in this study. Furthermore, there was no additional benefit in the outcome when the number of cycles was increased. The aforementioned studies did not assess the volume of opening, the permeability, or the reversibility timeline of BBB opening, rendering a direct comparison with those studies impossible. This study provides further insight in the underlying physiology for a range of acoustic parameters that have been shown to play a critical role in BBB opening.

The effect of the polydispersity of the bubbles used, compared with what has been previously reported for monodispersed microbubbles (1 to 2, 4 to 5, and 6 to 8 μm in diameter) at similar acoustic parameters [15], [16] should be taken into account. First, in those studies, it was shown that only the 4 to 5 μm and 6 to 8 μm bubbles were capable of inducing physiologic changes (permeability and BBB opening volume) at 100 cycles and 0.30 MPa, whereas the 1 to 2 μm mono-dispersed microbubbles could not. This could be attributed to the fact that, although it is highly polydisperse, the Definity mean diameter (1.1 to 3.3 μm) falls closer to the range of the 1 to 2 μm bubbles previously studied. Also, when the higher pressures of 0.45 MPa and 0.60 MPa were used, the permeability, the volume of opening, and the reversibility timeline at 6.7 μs with Definity were similar to what has been reported for the 1 to 2 μm bubbles [15], [16], and significantly lower than what has been reported for the 4 to 5 μm and 6 to 8 μm bubbles. These results suggest that the higher range of diameters—larger than 2 μm—contained in the poly-dispersed dose of Definity injected before sonication, were not sufficient to increase the bioeffects and efficacy of Definity above the level that the 1 to 2 μm mono-dispersed bubbles were shown to achieve, because their effect on the BBB opening permeability, volume, and reversibility timeline are quite similar.

In this study, a linear relationship was established between the time required for BBB closing and the volume of opening. It was found that the time required for closing increased monotonically. These results indicate that the duration of the induced BBB opening could be predicted based on the volume of opening after a single sonication, in agreement with previous reports [16]. The relation between the average permeability changes and the time of closing was not found to have a correlation that would allow K_{trans} to be reliable for closing prediction.

In contrast with the previously reported K_{trans} measurement methods developed by our group [15], in this study, the average K_{trans} was estimated over a VOI of 52 mm^3 which overlapped with the targeted region, instead of a small circular region of 1 mm in diameter, identical to the VOI where V_{BBB} was measured. The differences among different groups did not change; however, this method effectively provided a better approximation of the K_{trans} because the changes in the whole BBB-opened volume were taken into account, avoiding overestimation of the K_{trans} caused by focusing within a smaller area. Additionally, the stacked histograms showing the volume of each K_{trans} cluster (Fig. 4) for all the combinations of PL and PNP tested were found to better illustrate the nonuniform distribution of K_{trans} changes within the opened region. It should be noted that cases with similar K_{trans} distributions also had similar closing timelines.

There are several limitations associated with this study. One limitation could be due to the MR sensitivity resolution. The resolution was optimized, but small BBB disruptions may still remain undetectable. Also, because DCE MR images were acquired, there was approximately a 1 h interval between the acquisition of the first MRI image and the FUS application, during which the volume of opening could have decreased, especially for the cases of minute disruptions. A similar limitation is associated with the detection of closing. The animals with detectable but small openings were imaged 8 h after sonication. The rest of the animals were imaged in 24-h intervals, i.e., the time that was reported as “time required for closing” could be overestimated within the range of the time interval between the final two consecutive MRI scans. Finally, the detection and characterization of BBB opening, and thus the closing timeline, is dependent on the size of the tracer used, as well as the experimental configuration of the study. In this study, K_{trans}, V_{BBB}, and closing timeline were associated with the contrast agent used, i.e., gadodiamide, which has a very low molecular weight (574 Da). Larger MR tracers may be associated with different timelines than those reported in this paper [24]. It should be noted that the correlation between K_{trans},

V_{BBB}, and closing timeline might not be valid under more complex experimental conditions, such as overlapping targets, different transducer configuration, etc.

V. Conclusion

In this longitudinal study, the dependence of the BBB permeability after opening, opening volume, and reversibility timeline on the acoustic pulse length and peak rarefactional FUS pressure was established. It was found that, with the use of Definity microbubbles at relatively low peak rarefactional pressures (0.3 MPa), a longer pulse length was required to induce BBB opening. When higher pressures were used, i.e., 0.45 and 0.60 MPa, short pulse lengths were found to be sufficient for opening, and an increase in the pulse length enhanced all BBB opening characteristics. It was also found that the duration of BBB opening was linearly proportional to the initial volume of opening. Finally, there was no histological damage detected in any of the animals studied, indicating that all methodology parameters used here fell within the safety window of the technique.

Acknowledgments

The authors wish to thank O. Olumolade, B.S. (biomedical engineering) for the histological specimen analysis at Columbia University, and S. Wang, Ph.D. (biomedical engineering), C. Chen, Ph.D. (biomedical engineering), and F. Marquet, Ph.D. (biomedical engineering) for their important input.

This study was supported in part by National Institutes of Health (NIH) grants R01EB009041 and 1R01AG038961.

References

1. Rubin LL, Staddon JM. The cell biology of the blood–brain barrier. Annu. Rev. Neurosci. 1999 Mar.vol. 22(no. 1):11–28. [PubMed: 10202530]
2. Abbott NJ, Ronnback L, Hansson E. Astrocyte-endothelial interactions at the blood–brain barrier. Nat. Rev. Neurosci. 2006 Jan.vol. 7(no. 1):41–53. [PubMed: 16371949]
3. Pardridge WM. The blood–brain barrier: Bottleneck in brain drug development. NeuroRx. 2005 Jan.vol. 2(no. 1):3–14. [PubMed: 15717053]
4. Hynynen K, McDannold N, Vykhodtseva N, Jolesz FA. Noninvasive MR imaging-guided focal opening of the blood–brain barrier in rabbits. Radiology. 2001 Sep.vol. 220(no. 3):640–646. [PubMed: 11526261]
5. Choi JJ, Pernot M, Brown TR, Small SA, Konofagou EE. Spatio-temporal analysis of molecular delivery through the blood–brain barrier using focused ultrasound. Phys. Med. Biol. 2007 Sep.vol. 52(no. 18):5509–5530. [PubMed: 17804879]
6. Yang F-Y, Fu W-M, Yang R-S, Liou H-C, Kang K-H, Lin W-L. Quantitative evaluation of focused ultrasound with a contrast agent on blood–brain barrier disruption. Ultrasound Med. Biol. 2007 Sep.vol. 33(no. 9):1421–1427. [PubMed: 17561334]
7. Liu H-L, Wai Y-Y, Chen W-S, Chen J-C, Hsu P-H, Wu X-Y, Huang W-C, Yen T-C, Wang J-J. Hemorrhage detection during focused-ultrasound induced blood–brain-barrier opening by using susceptibility-weighted magnetic resonance imaging. Ultrasound Med. Biol. 2008 Apr.vol. 34(no. 4):598–606. [PubMed: 18313204]
8. McDannold N, Vykhodtseva N, Hynynen K. Blood–brain barrier disruption induced by focused ultrasound and circulating preformed microbubbles appears to be characterized by the mechanical index. Ultrasound Med. Biol. 2008 May; vol. 34(no. 5):834–840. [PubMed: 18207311]
9. Bing KF, Howles GP, Qi Y, Palmeri ML, Nightingale KR. Blood–brain barrier (BBB) disruption using a diagnostic ultrasound scanner and Definity in mice. Ultrasound Med. Biol. 2009 Aug.vol. 35(no. 8):1298–1308. [PubMed: 19545939]
10. McDannold N, Vykhodtseva N, Hynynen K. Effects of acoustic parameters and ultrasound contrast agent dose on focused-ultrasound induced blood–brain barrier disruption. Ultrasound Med. Biol. 2008 Jun.vol. 34(no. 6):930–937. [PubMed: 18294757]

11. Choi JJ, Selert K, Gao Z, Samiotaki G, Baseri B, Konofagou EE. Noninvasive and localized blood–brain barrier disruption using focused ultrasound can be achieved at short pulse lengths and low pulse repetition frequencies. J. Cereb. Blood Flow Metab. 2011 Feb.vol. 31(no. 2):725–737. [PubMed: 20842160]
12. Choi JJ, Selert K, Vlachos F, Wong A, Konofagou EE. Noninvasive and localized neuronal delivery using short ultrasonic pulses and microbubbles. Proc. Natl. Acad. Sci. USA. 2011 Oct.vol. 108(no. 40):16539–16544. [PubMed: 21930942]
13. Chopra R, Vykhodtseva N, Hynynen K. Influence of exposure time and pressure amplitude on blood–brain-barrier opening using transcranial ultrasound exposures. ACS Chem Neurosci. 2010 May; vol. 1(no. 5):391–398. [PubMed: 20563295]
14. Choi JJ, Feshitan JA, Baseri B, Wang S, Tung Y-S, Borden MA, Konofagou EE. Microbubble-size dependence of focused ultrasound-induced blood–brain barrier opening in mice in vivo. IEEE Trans. Biomed. Eng. 2010 Jan.vol. 57(no. 1):145–154. [PubMed: 19846365]
15. Vlachos F, Tung Y-S, Konofagou E. Permeability dependence study of the focused ultrasound-induced blood–brain barrier opening at distinct pressures and microbubble diameters using DCE-MRI. Magn. Reson. Med. 2011 Sep.vol. 66(no. 3):821–830. [PubMed: 21465543]
16. Samiotaki G, Vlachos F, Tung Y-S, Konofagou EE. A quantitative pressure and microbubble-size dependence study of focused ultrasound-induced blood–brain barrier opening reversibility in vivo using MRI. Magn. Reson. Med. 2012; vol. 67(no. 3):769–777. [PubMed: 21858862]
17. Tung Y-S, Vlachos F, Feshitan JA, Borden MA, Konofagou EE. The mechanism of interaction between focused ultrasound and microbubbles in blood–brain barrier opening in mice. J. Acoust. Soc. Am. 2011 Nov.vol. 130(no. 5):3059–3067. [PubMed: 22087933]
18. O'Reilly MA, Waspe AC, Ganguly M, Hynynen K. Focused-ultrasound disruption of the blood–brain barrier using closely-timed short pulses: Influence of sonication parameters and injection rate. Ultrasound Med. Biol. 2011 Apr.vol. 37(no. 4):587–594. [PubMed: 21376455]
19. Park J, Zhang Y, Vykhodtseva N, Jolesz FA, McDannold NJ. The kinetics of blood brain barrier permeability and targeted doxorubicin delivery into brain induced by focused ultrasound. J. Control. Release. 2012 Aug.vol. 162(no. 1):134–142. [PubMed: 22709590]
20. Goertz DE, de Jong N, van der Steen AFW. Attenuation and size distribution measurements of Definity and manipulated Definity populations. Ultrasound Med. Biol. 2007 Sep.vol. 33(no. 9): 1376–1388. [PubMed: 17521801]
21. Stapleton S, Goodman H, Zhou Y-Q, Cherin E, Henkelman RM, Burns PN, Foster FS. Acoustic and kinetic behaviour of Definity in mice exposed to high frequency ultrasound. Ultrasound Med. Biol. 2009 Feb.vol. 35(no. 2):296–307. [PubMed: 18950930]
22. Tofts PS, Kermode AG. Measurement of the blood–brain barrier permeability and leakage space using dynamic MR imaging. 1. Fundamental concepts. Magn. Reson. Med. 1991 Feb.vol. 17(no. 2):357–367. [PubMed: 2062210]
23. Tung Y-S, Vlachos F, Choi JJ, Deffieux T, Selert K, Konofagou EE. In vivo transcranial cavitation threshold detection during ultrasound-induced blood–brain barrier opening in mice. Phys. Med. Biol. 2010 Oct.vol. 55(no. 20):6141–6155. [PubMed: 20876972]
24. Marty B, Larrat B, Van Landeghem M, Robic C, Robert P, Port M, Le Bihan D, Pernot M, Tanter M, Lethimonnier F, Mériaux S. Dynamic study of blood–brain barrier closure after its disruption using ultrasound: A quantitative analysis. J. Cereb. Blood Flow Metab. 2012 Oct.vol. 32(no. 10): 1948–1958. [PubMed: 22805875]

Biographies

Gesthimani (Mania) Samiotaki received her diploma in electrical and computer engineering in 2009, and majored in electronics, systems, and signals. During her undergraduate studies, she did volunteer research on biomedical image processing and simulation of physiological systems. In fall 2009, she enrolled in Columbia University's Ph.D. program in biomedical engineering. Her research interests include noninvasive, localized delivery of drugs and potential therapeutic agents using ultrasound, working at the Elasticity Imaging and Ultrasound Laboratory (UEIL).

Elisa E. Konofagou received her B.S. degree in chemical physics from Université de Pierre et Marie Curie, Paris VI in Paris, France, and her M.S. degree in biomedical engineering from the Imperial College of Physics, Engineering, and Medicine in London, UK, in 1992 and 1993, respectively. In 1999, Dr. Konofagou received her Ph.D. degree in biomedical engineering from the University of Houston, Houston, TX, for her work on multidimensional elastography for breast cancer diagnosis at the University of Texas Medical School, Houston, TX, then pursued her postdoctoral work in elasticity-based monitoring of ultrasound therapy at Brigham and Women's Hospital, Harvard Medical School, Boston, MA. Dr. Konofagou is currently an associate professor of biomedical engineering and radiology and Director of the Ultrasound and Elasticity Imaging Laboratory at Columbia University, New York. Her main interests are in the development of novel elasticity imaging techniques and therapeutic ultrasound methods, such as myocardial elastography, breast elastography, ligament elastography, harmonic motion imaging, and ultrasound-induced brain drug delivery, with several clinical collaborations in the Columbia Presbyterian Medicine Center, New York. Dr. Konofagou is a technical committee member of the Acoustical Society of America and a technical standards committee member of the American Institute of Ultrasound in Medicine. She has served on peer review committees for the National Institutes of Health, the National Aeronautics and Space Administration, and the National Science Foundation. She also serves as an associate editor for the journal *Medical Physics* and as an editorial board member of the *Ultrasound in Medicine and Biology* journal, and is the recipient of several awards, including awards from the Acoustical Society of America, the American Heart Association, the American Institute of Ultrasound in Medicine, the National Institutes of Health, the National Science Foundation, the Radiology Society of North America, and the Wallace H. Coulter Foundation. She is also a member of the IEEE Ultrasonics, Ferroelectrics, and Frequency Control Society; the International Society of Therapeutic Ultrasound; the Acoustical Society of America; the American Institute of Ultrasound in Medicine; and the American Heart Association.

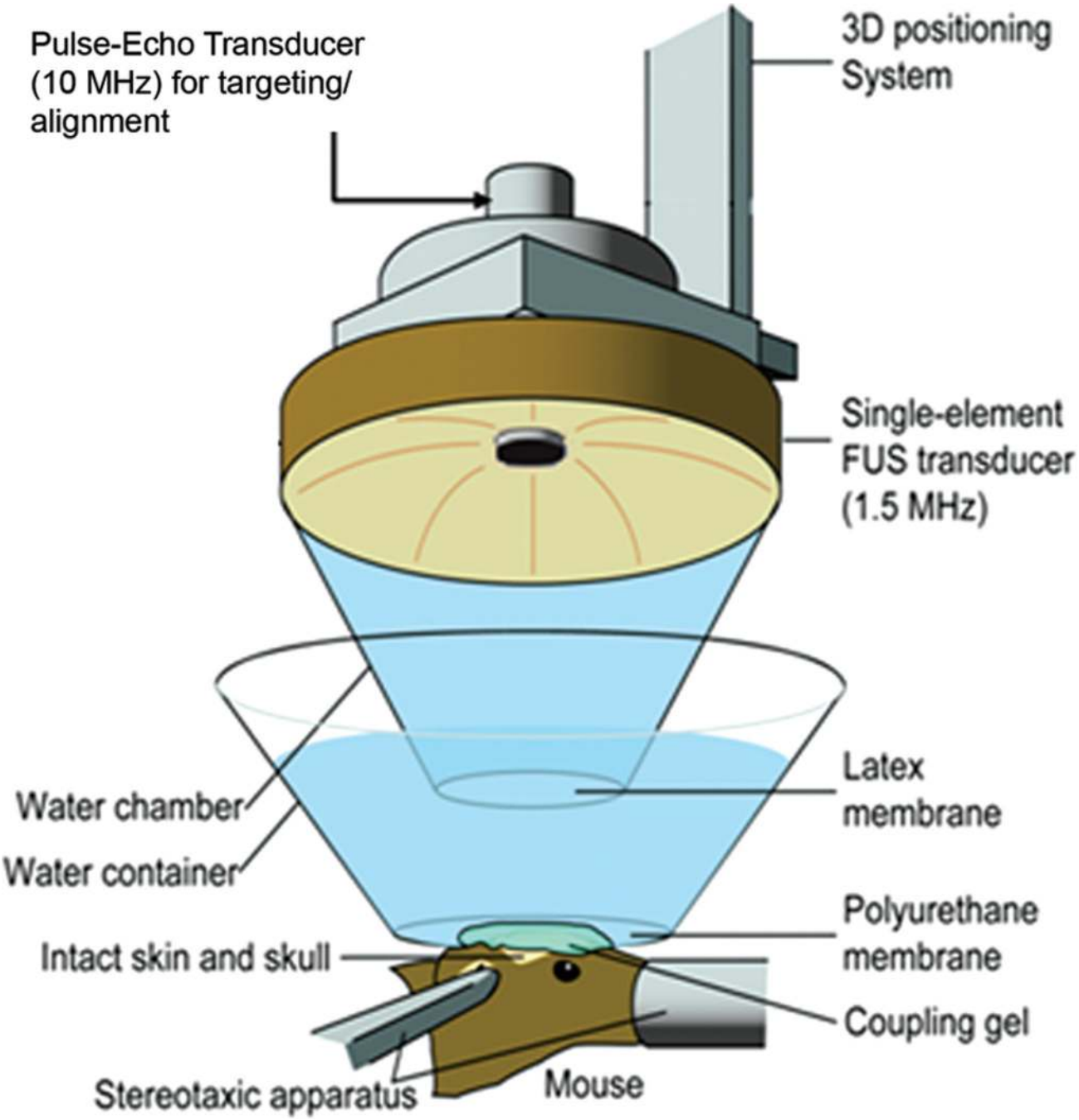

Fig. 1.
Experimental setup.

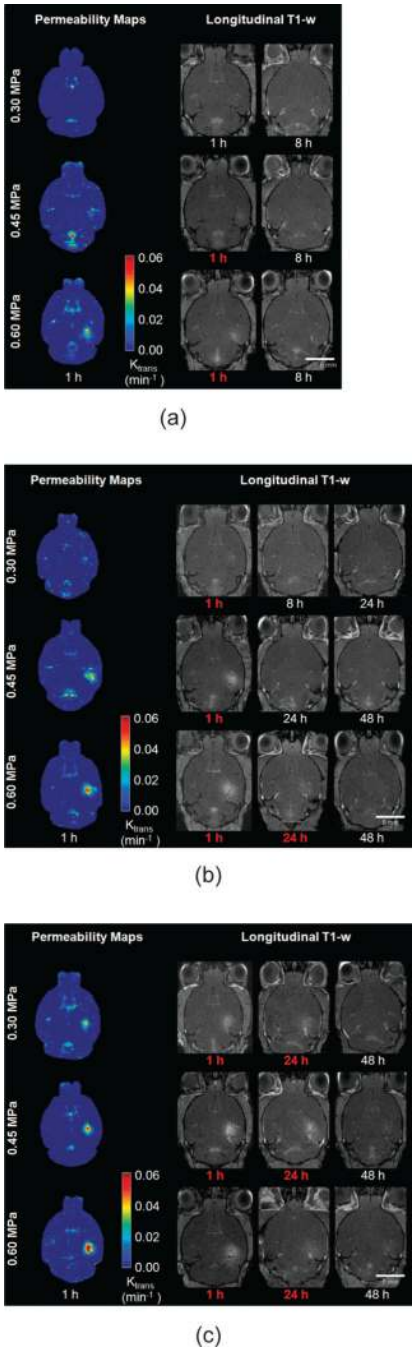

Fig. 2.

Horizontal permeability maps after focused ultrasound, followed by longitudinal T1-weighted images showing the reversibility timeline for all peak negative acoustic pressures with a pulse length of (a) 67 μs, (b) 0.67 ms and (c) 6.7 ms. Signal enhancement in the blood–brain barrier (BBB) opened region resulting from diffusion of gadodiamide through the BBB is observed in the sonicated region, which was overlapping with the right hippocampus. Red font color denotes that BBB opening was detected.

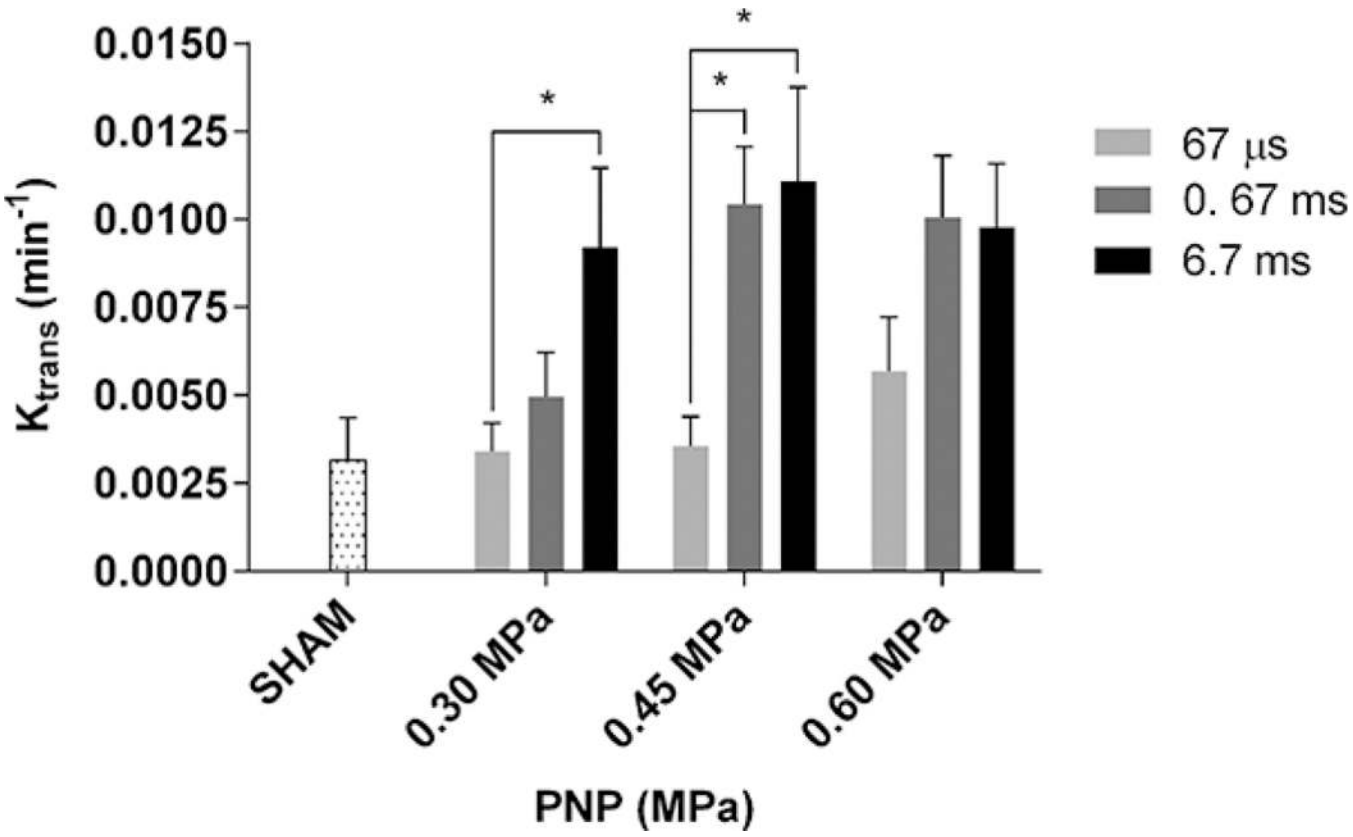

Fig. 3.

K_{trans} averaged across the entire sonicated area at different peak negative acoustic pressures (PNPs) and pulse lengths. Error bars are equal to one standard deviation. Asterisks (*) denote statistical significance ($p < 0.05$). The permeability of the sham group is also shown (0.0030 ± 0.0007 min^{-1}). The average K_{trans} in the 0.30 MPa/67 µs, 0.30 MPa/0.67 ms, and 0.45 MPa/67 µs cases were not statistically different from the sham.

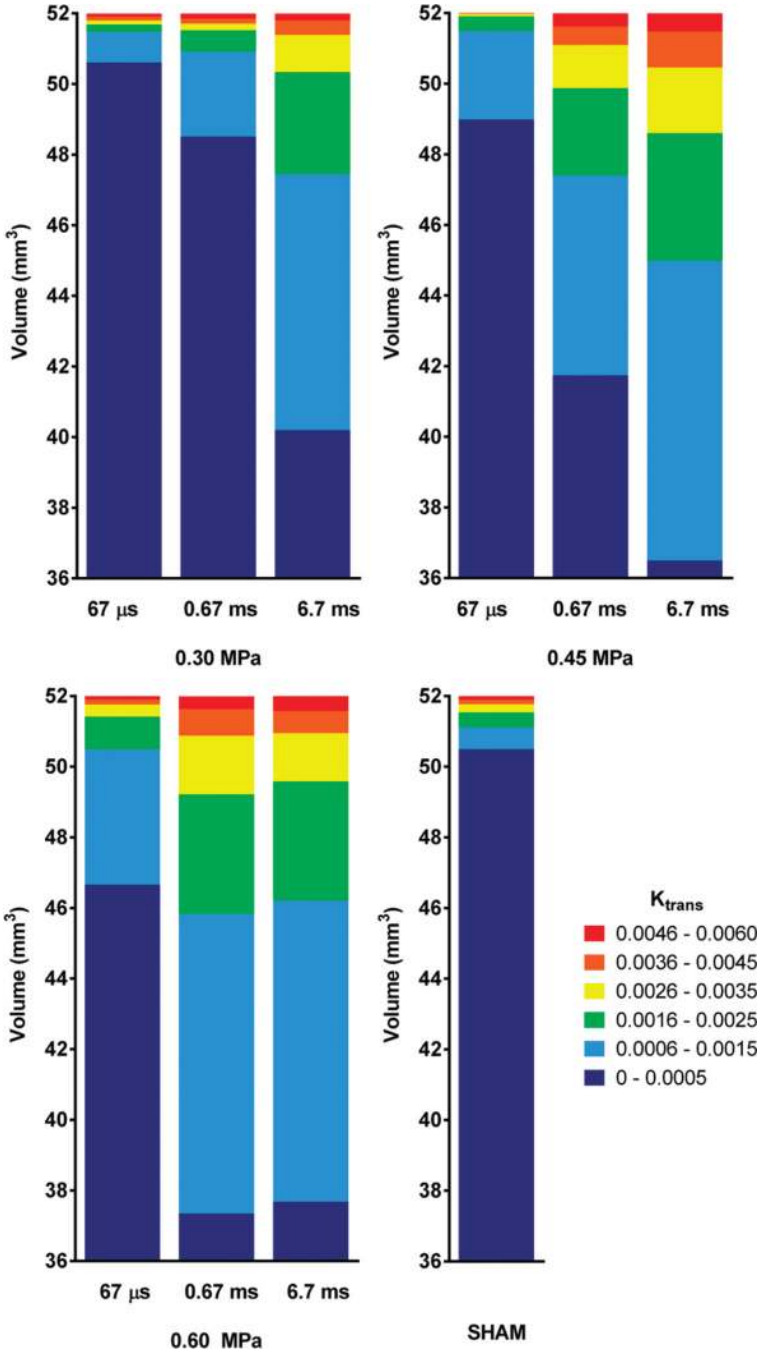

Fig. 4.

Stacked histograms of K_{trans} values. K_{trans} values of all permeability maps created were grouped into six clusters (i.e., 0 to 0.005, 0.006 to 0.015, 0.016 to 0.025, 0.026 to 0.035, 0.036 to 0.045, and 0.046 to 0.060 min^{-1}), and the average volume of each cluster is shown for all peak negative acoustic pressures and pulse lengths.

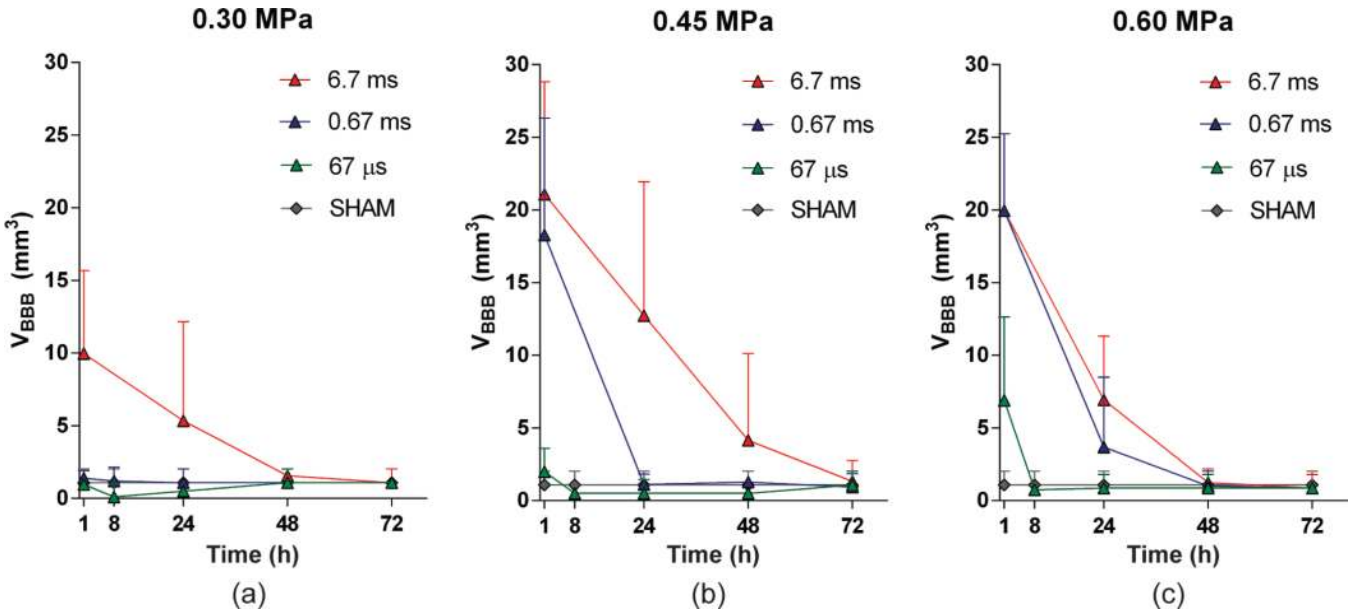

Fig. 5.

Blood–brain barrier (BBB) opening volume for each group, with all pulse lengths and peak negative acoustic pressures of (a) 0.30 MPa, (b) 0.45 MPa, and (c) 0.60 MPa. Error bars correspond to standard deviation (S.D.) across different mice. There was no opening detected at 67 μs/0.30 MPa. Closing occurred within 8 h for the 67-μs/0.45-MPa, 67-μs/0.60-MPa, and 0.67-ms/0.30-MPa cases. Closing occurred within 24 to 48 h for the 0.67-ms/0.45-MPa and 6.7-ms/0.30-MPa cases. Finally, closing occurred within 48 to 72 h for the 6.7-ms/0.45-MPa, 6.7-ms/0.60-MPa, and 0.67-ms/0.60-MPa cases.

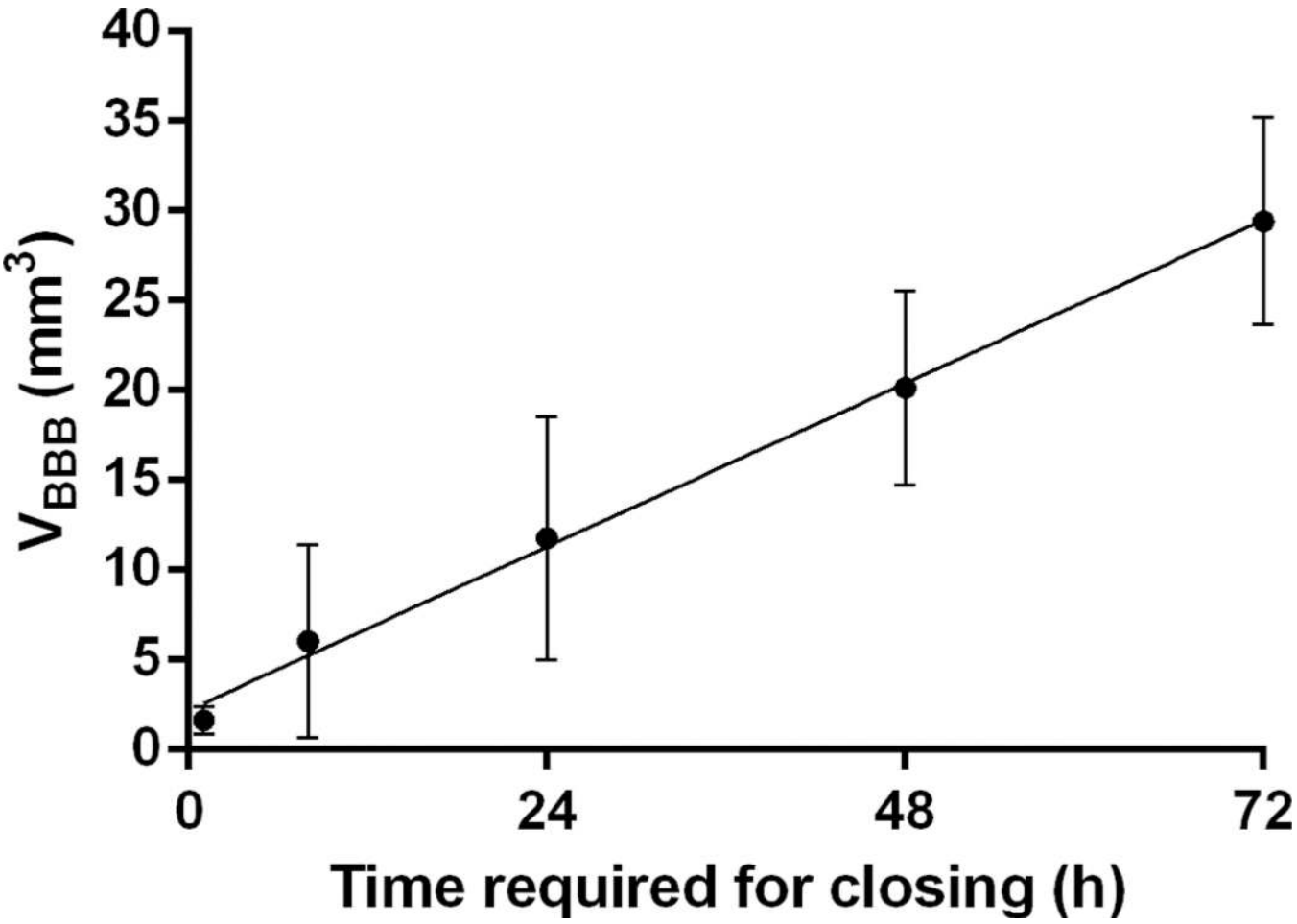

Fig. 6.
Correlation of the volume of opening (V_{BBB}) 1 h after focused ultrasound and the time required for closing. Linear regression shows good correlation ($R^2 = 0.77$). The reversibility of blood–brain barrier opening was measured to have a volume decay rate of 11.4 ± 4.0 mm^3 per day.

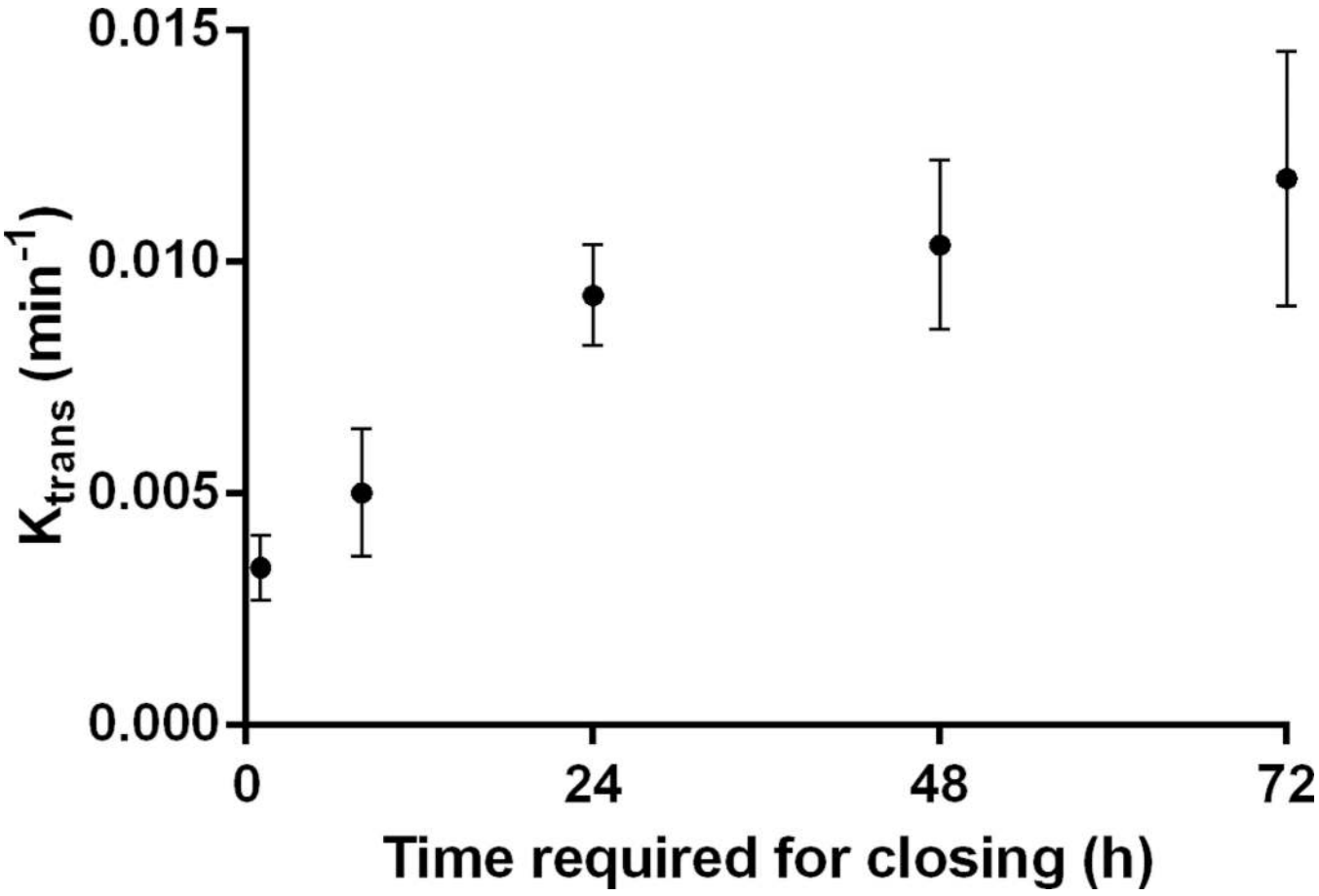

Fig. 7.
Average K_{trans} 1 h after focused ultrasound versus the time required for closing.

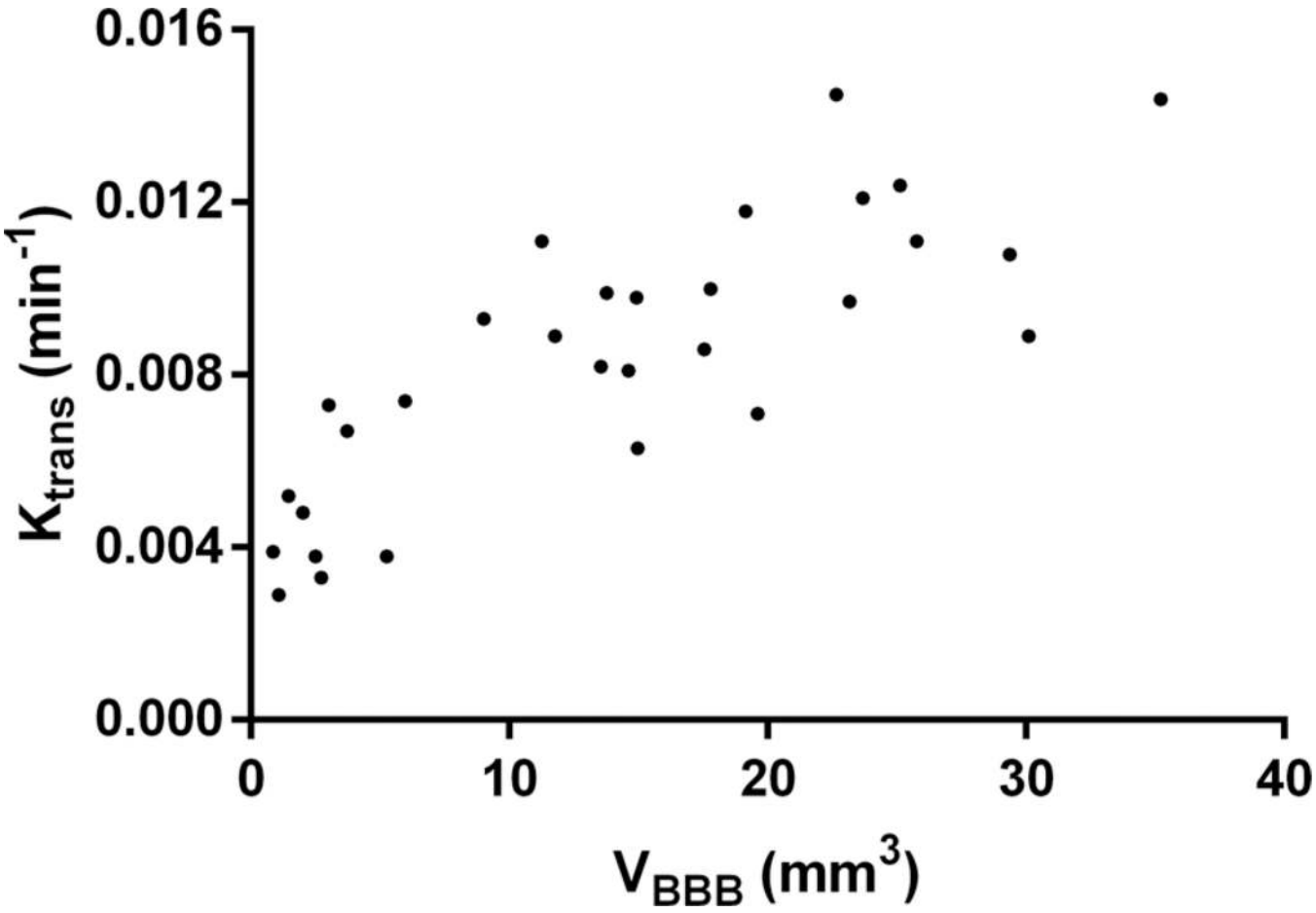

Fig. 8.
Scatter plot of the K_{trans} versus V_{BBB} measured in the same volume-of-interest 1 h after opening. A linear fit shows a good correlation ($R^2 = 0.74$).

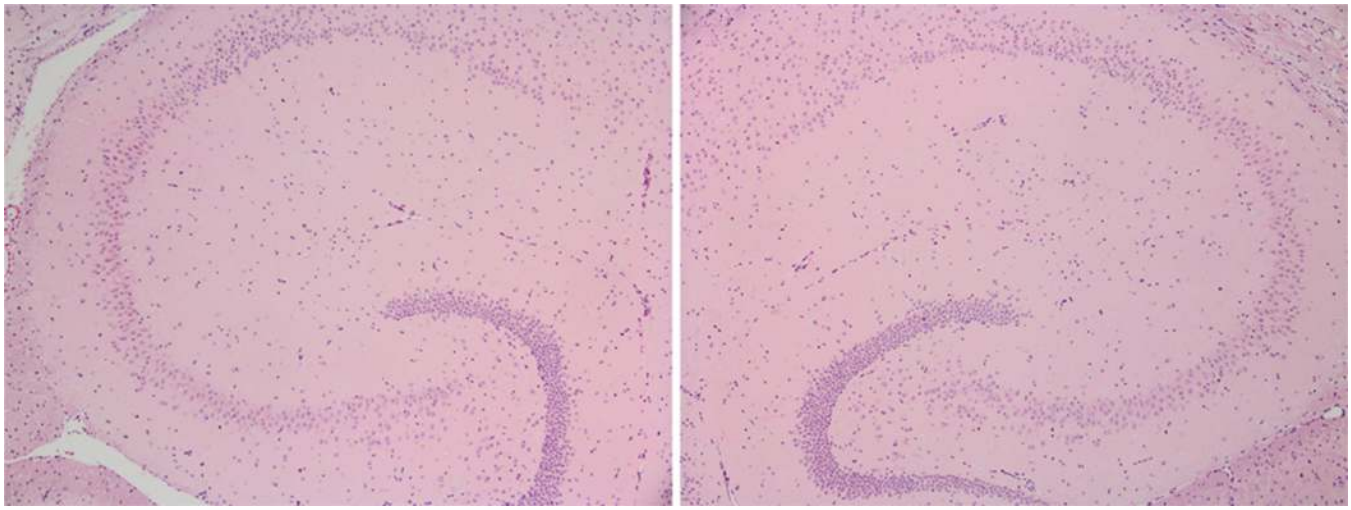

Fig. 9.

Hematoxylin and eosin (H&E)-stained horizontal slices of 6 μm thickness magnified (4×) in the area of the (left) left and (right) right hippocampus for a case of 6.7 ms pulse length and 0.60 MPa, i.e., the highest focused ultrasound energy case. No damage was detected in any of the mice in the study.